Laguerre and Hermite Soliton Clusters in Nonlocal Nonlinear Media

Daniel Buccoliero,[1,2] Anton S. Desyatnikov,[1] Wieslaw Krolikowski,[2] and Yuri S. Kivshar[1]

[1]*Nonlinear Physics Center, Research School of Physical Sciences and Engineering, Australian National University, Canberra, ACT 0200, Australia*

[2]*Laser Physics Center, Research School of Physical Sciences and Engineering, Australian National University, Canberra, ACT 0200, Australia*

(Received 29 November 2006; published 1 February 2007)

We introduce novel classes of higher-order spatial optical solitons in analogy with Laguerre-Gaussian and Hermite-Gaussian linear eigenmodes. We reveal that stable higher-order optical solitons can exist in nonlocal nonlinear media in the various forms of soliton necklaces and soliton matrices. Modulational instability can lead to nontrivial transformations between energetically close solitons with different symmetries through the intermediate states resembling generalized Hermite-Laguerre-Gaussian modes.

DOI: 10.1103/PhysRevLett.98.053901 PACS numbers: 42.65.Tg, 42.65.Hw, 42.65.Pc

Recent experimental observations of the existence, stability, and interactions of spatial optical solitons in nematic liquid crystals [1] and lead glasses [2] stimulate further theoretical studies of intriguing properties of the self-trapped optical beams in media with nonlocal nonlinear response. Some earlier theoretical results described the basic properties of nonlocal optical solitons [3], as well as analyzed the stabilization against symmetry breaking instability of vortex solitons [4], rotating dipole solitons [5–7], and azimuthons [8–10]. Very recently, novel experimental results on the generation of dipole, tripole, and quadrupole solitons, as well as necklace beams [11] have been presented [12].

In any realistic nonlinear medium with a local response [13], higher-order optical solitons and vortices are known to be unstable [14]. Nonlocality can suppress the azimuthal instability, and it can also support multisoliton bound states [15] and otherwise nonstationary structures, such as dipole solitons. Since the ringlike solitons resemble the structure of the Laguerre-Gaussian (LG) linear modes, and the tripole solitons resemble the Hermite-Gaussian (HG) optical beams, it is natural to ask whether the counterparts of other well-known linear optical modes [16,17] exist in nonlinear media. In particular, we are interested in exploring what kind of soliton ''rings'' and ''matrices'' can be supported and stabilized by nonlocal nonlinear medium.

In this Letter, we start from a set of linear optical LG and HG waveguide modes to construct higher-order spatial solitons in nonlocal nonlinear media in the form of soliton clusters: necklaces and matrices. We identify those novel types of solitons as Laguerre-nonlocal (LN_{nm}) and Hermite-nonlocal (HN_{nm}) spatial solitons with distinct differences in their symmetry. In this approach, the multiple-ring soliton necklaces LN_{nm} are characterized by the number of radial nodes n and the topological index m. Similarly, the indices of the soliton matrices HN_{nm} determine the number of nodes in two orthogonal directions. Using the variational approach [18] and numerical minimization of the error functional [19], we find analytically and numerically broad classes of higher-order localized states and demonstrate that only a few of them are energetically separated from each other. In general, localized states with different symmetries coexist, i.e., they have the same power and energy. While the lower-order energetically separated states (e.g., dipoles) become stable when the nonlocality parameter (or the beam power) exceeds a certain threshold value, the power of the higher-order solitons can coincide and nontrivial effects of revivals and transformations are observed.

We consider the propagation of paraxial optical beams with scalar field envelope E in the medium with nonlocal Gaussian response described by the nonlinear Schrödinger (NLS) equation [13], $i\partial_z E = \delta\mathcal{H}/\delta E^*$ being its Hamiltonian representation. Stationary states can be found in a generic form as $E(x, y, z) = U(x, y)\exp(ikz)$ with the Lagrangian $\mathcal{L} = -kP - \mathcal{H}$, where the integrals of motion are the power, $P = \int |U|^2 d\mathbf{r}$, and Hamiltonian,

$$\mathcal{H} = \int\left(|\nabla U|^2 - \frac{1}{2}|U|^2\int e^{-|\mathbf{r}-\mathbf{r}'|^2}|U(\mathbf{r}')|^2 d\mathbf{r}'\right)d\mathbf{r}. \quad (1)$$

Physical variables absorb the transverse scale of nonlocality σ as follows, $\tilde{z} = z\sigma^2$, $\tilde{\mathbf{r}} = \mathbf{r}\sigma$, and $\tilde{E} = \sqrt{\pi}E/\sigma$. Note that the power, $\tilde{P} = \pi P$, and the orbital angular momentum, $\tilde{M} = \pi M$, do not depend on σ, here $M = \mathrm{Im}\int U^*|\mathbf{r}\times\nabla U|d\mathbf{r}$. However, the soliton constant and the Hamiltonian scale as $\tilde{k} = k/\sigma^2$ and $\tilde{\mathcal{H}} = \pi\mathcal{H}/\sigma^2$.

One-dimensional solitons.—In local media, the only stationary scalar solution is a fundamental soliton, while nonlocality allows us to compensate the soliton repulsion stabilizing multihump solitons [20], similar to nonlinear modes in confining potential [21]. We notice that in the linear limit $U \to 0$, such modes correspond to the diffracting HG modes

$$U_n(x) = A\exp(-x^2/2a^2)H_n(x/b), \quad (2)$$

where the integer index n determines the number of nodes across the Gaussian envelope and $H_n(t) = (-1)^n e^{t^2}d^n e^{-t^2}/dt^n$ is the Hermite polynomial. We use Eq. (2) as the ansatz in the nonlinear problem (1) and

derive variational solutions using the standard Ritz minimization procedure [18] with the variational parameters A, a, and b ($b \equiv 1$ for $n = 0, 1$). Numerical solutions for different n are shown in Fig. 1.

Laguerre-Nonlocal solitons.—The variational ansatz for the LN_{nm} solitons can be constructed using the separation of variables in the cylindrical coordinates, $U(x, y) = R_{nm}(r)(\cos m\varphi + ip \sin m\varphi)$, where the radial envelope R_{nm} with n nodes solves the nonlinear ordinary differential equation [5]. Parameter $p \in [0, 1]$ determines the depth of azimuthal modulation ($p \equiv 1$ for $m = 0$) as well as the angular momentum, $M = 2mpP/(1 + p^2)$. Further simplification of this method was implemented in Refs. [7,10] for the radially symmetric vortices with $p = 1$, and here we extend it to the general case $p \leq 1$. Radial envelope is sought in the form

$$R_{nm}(x, y) = Ar^m \exp(-r^2/2a^2) L_n^m(r^2/b^2)$$

with the generalized Laguerre polynomial $L_n^m(t) = \frac{1}{n!} t^{-m} e^t d^n(t^{n+m} e^{-t})/dt^n$. The results in terms of the soliton power P vs propagation constant k and Hamiltonian $\mathcal{H}$ vs P are plotted in Fig. 2(a) for several different LN_{nm} solitons.

The singular LN_{nm} solitons with $m \neq 0$ occupy the continuous bands in the diagrams in Fig. 2(a) which we obtain by varying the modulation parameter p. Thus, soliton necklaces with $p = 0$ and vortex solitons with $p = 1$ form the lower and the upper-energy edges of the bands. For the lowest-order single-ring LN_{0m} necklaces the bands are quite narrow, while their width diverges quickly with the number of rings. Note that solitons with different values of p are physically separated within the band by the conservation of the angular momentum M.

Hermite-nonlocal solitons.—Separation of variables $U(x, y) = X(x)Y(y)$ in Eq. (1) leads to two coupled one-dimensional subsystems for the envelopes X and Y which can be, in general, complex. Indeed, the more general family of the HN solitons will include singular solutions with nontrivial phase and nonzero angular momentum, similar to the LN solitons. However, their structure is expected to contain multiple phase dislocations and, for simplicity, here we consider only real envelopes $X(x) = U_n(x)$ and $Y(y) = U_m(y)$ given by Eq. (2) with independent parameters. Deriving variational equations, we establish the relations between the parameters of one-dimensional envelopes which give the final parameters of two-dimensional "soliton matrices." Variational solution serves as a good guess for further use in numerical relaxation method; two examples of exact HN_{nm} solitons are presented in Figs. 2(e) and 2(f). Exact envelopes $U(x, y)$ were obtained with relaxation procedure [19] which consist of numerical minimization of the error functional, $\int |f|^2 d\mathbf{r}$, generated at the right hand side of stationary NLS equation, $kU_{\mathrm{tr}} + \delta\mathcal{H}/\delta U_{\mathrm{tr}} = f$, so that $f \to 0$ when the trial function approaches solution $U_{\mathrm{tr}} \to U$.

Coexistence of HN and LN solitons.—We introduced above two distinct families of solutions, but the comparison of two $\mathcal{H}(P)$ diagrams in Figs. 2(a) and 2(b) suggests that it is not always possible to separate them energetically and to distinguish between "lower-" and "higher-order" solitons. For the radially symmetric LN-solitons with $p = 1$, the variational solutions provide a very good approximation of the integral characteristics [7] (power and Hamiltonian), and here we confirm this result for soliton necklaces LN_{nm} with $p = 0$ and low-order soliton matrices HN_{nm}. Indeed, for a given value of k, the power of exact solutions in Fig. 2(c)–2(f) differs from variationally predicted values in Figs. 2(a) and 2(b) within a remarkable 1% of accuracy, while differences in Hamiltonian values are within 10%.

However, for higher-order HN solitons, such as HN_{22} soliton matrix in Fig. 3 (top), the profiles of exact solutions deviate from our ansatz. For low power in Fig. 3(a), the HN_{22} soliton attains a shape of a square array of 9 out-of-phase spatially well-separated solitons, the square being stretched by its corners. At intermediate powers, as in Fig. 3(b), the shape is fairly close to the HG ansatz. With further increase of the power, the square geometry is

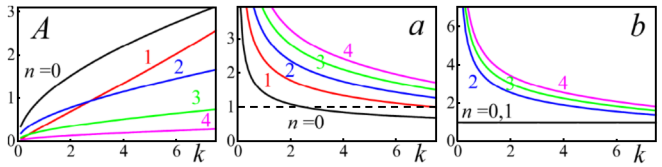

FIG. 1 (color online). Variational parameters of the one-dimensional HN_n solitons, Eq. (2). The index n is shown next to the curves.

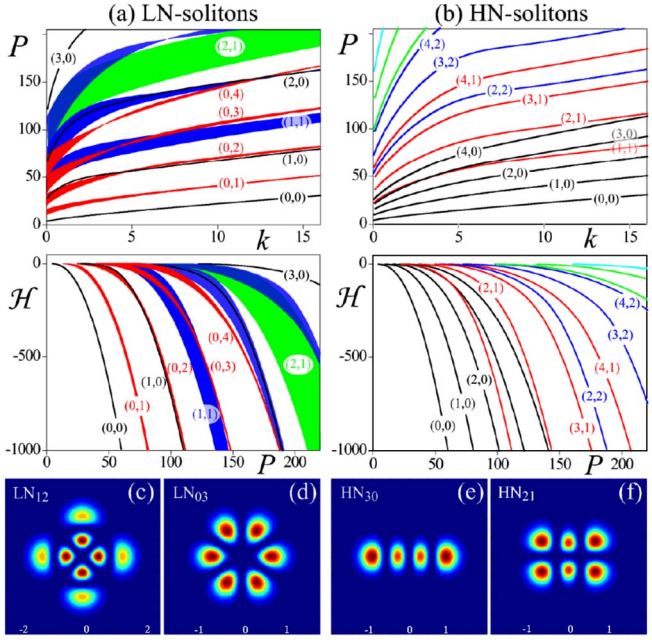

FIG. 2 (color online). (a,b) Variational diagrams and (c–f) exact profiles for (a, c, d) Laguerre- and (b, e, f) Hermite-nonlocal solitons. Solitons in (c–f) have the power $P \simeq 200$.

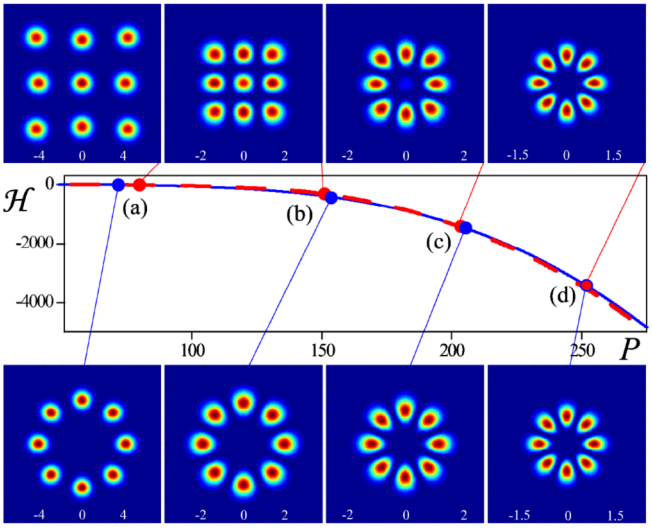

FIG. 3 (color online). Coexistence of HN_{22} matrix (top row, dashed line) and LN_{04} necklace (bottom row, solid line). Variational (lines) and exact (dots and profiles) solutions are shown for $k = 2.12$ (a), 11.5 (b), 30.34 (c), and 54.45 (d).

gradually lost [there is still a nonzero peak at the origin of the "matrix" HN_{22} in (c)], and at approximately $P \geq 250$, the soliton matrix HN_{22} disappears by "fusion" with 8-soliton necklace LN_{04} (see Fig. 3(d)). The change of the geometry of the HN_{22} solutions slows down our relaxation procedure; it is in contrast to the LN_{04} solitons in Fig. 3 (bottom), for which the variational ansatz provides an excellent approximation.

Two major conclusions can be drawn from Fig. 3. First, the high-order HN_{nm} solitons can exist in a limited domain ($P \leq P_{\max}$ and $k \leq k_{\max}$), which implies that there should be an upper limit for the number of solitons in the matrix, $N \leq N_{\max}$, here $N \equiv (n+1)(m+1)$. Second, despite differences in their geometry, the soliton matrix HN_{22} and soliton necklace LN_{04} belong, in fact, to the same general family of solitons.

For deeper understanding of the soliton coexistence, we recall the so-called generalized Hermite-Laguerre-Gaussian $HLG_{nm}(x, y; \alpha)$ modes in linear media [16]. Two sets of modes, the LG and HG beams, appear as two particular realizations of the HLG family attained for the limiting values of the parameter α. The idea of such generalization is that for the intermediate values of α, any HLG beam also represents a self-similar and structurally stable solution. Thus, we expect that, similar to the LN and HN solitons, there is a greater variety of nonlinear states parameterized by some structural parameter, such as modulational parameter p for the LN-solitons. Indeed, while our ansatz $\sim \cos m\varphi + ip \sin m\varphi$ [5] represents exactly the HLG_{nm} modal beam for $n = 0$ and $m = 1$ only [16], it is no longer the case for higher-order HLG modes. Particularly important will be to trace the continuation $M > 0$ for HN solitons which is offered by HLG modes with astigmatic transformations through the parameter α. The results on nonlinear generalized HLG beams will be presented elsewhere.

Mode conversion.—We use variational solutions as input profiles for the direct simulation of the beam propagation. At the initial stage, the beams oscillate slightly [6] because the variational profiles differ from the stationary solutions. When the soliton is stable, these oscillations (internal modes) slowly decay with propagation [5]. In the region of instability, we observe different scenarios of soliton dynamics, depending on their power. Apart from the breakup into several fundamental solitons at low power (as in local media) or irregular dynamics for stronger nonlocality, we describe below the quasiperiodic dynamics with soliton revivals and mode transformations.

First, we consider the transformation of the radially symmetric LN_{10} soliton into the structure resembling LN_{02} (or HN_{11}) quadrupole [see column (c) of Fig. 4]. The corresponding $\mathcal{H}(P)$ diagram in Fig. 4(a) features crossing of these two modes, and also indicates that the double-ring fundamental soliton LN_{10} exists always within the band of the quadrupole mode LN_{02}. We argue that energy crossing of the two states is responsible for the mutual transformation of these two modes observed in Ref. [7]. As the next step, we simulate the propagation of the quadrupole soliton in Fig. 4(d) and observe remarkable

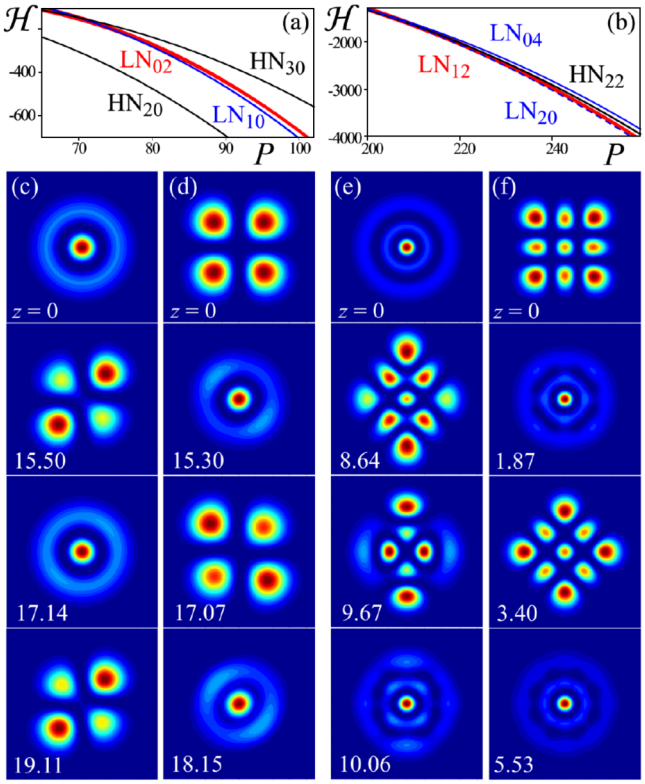

FIG. 4 (color online). (a,b) Energy crossings chosen from the overlapping of two ($\mathcal{H}$, P) diagrams in Figs. 2(a) and 2(b). Examples of the propagation dynamics of (c) LN_{10} soliton with $P = 100$, (d) HN_{11} (quadrupole, same as LN_{02}) with $P = 75$, (e) LN_{20} with $P = 250$, and (f) HN_{22} with $P = 210$.

similarities between the two; the latter includes periodic transformations to the LN_{02} as well as revivals. Thus, when two states cross, we expect and indeed observe mutual transformations of solitons, despite the sharp differences of their symmetry and stability.

The diagram in Fig. 4(a) also includes the ''four-soliton vector'' HN_{30} and the tripole HN_{20} [12]. In the region of powers in Fig. 4(a), both soliton vectors disintegrate into repelling fundamental solitons; thus, we do not observe any transformations involving other states. For higher powers, the soliton vectors become energetically isolated and stable; note however that the tripole was shown to be unstable in media with thermal nonlinearity [10].

Next, we show in Figs. 4(b), 4(e), and 4(f) another example of soliton transformations. The energy diagrams of four different solitons in Fig. 4(b) remain very close after crossing, and consequently, we observe mutual transformations among three of them. Namely, a double-ring fundamental soliton LN_{20} in Fig. 4(e) undergoes complex dynamics where we could clearly identify periodic appearance of LN_{12} and HN_{22} states, followed by soliton revival. Similarly, the 3×3 ''soliton matrix'' HN_{22} in Fig. 4(f) transforms quasiperiodically to LN_{20} mode. Interestingly, we do not observe appearance of the eight-soliton necklace LN_{04}, while its transformation to the matrix HN_{22} takes place (e.g., for $P = 220$, not shown), before it became stable at $P \geq 250$ [cf. Figure 3(b)]. Note also that crossed states appear largely distorted by their internal vibrations. This observation suggests that overlapping of soliton internal modes, in addition to crossing of stationary states, must determine mutual soliton transformations.

We considered above the transformations between states with zero vorticity as the simplest example. Because of the conservation of angular momentum, the transformations between singular states will be accompanied by their rotation, as in Ref. [5]. Furthermore, it is expected that a variety of ''solitonic molecules'' or clusters will increase dramatically in the rotating grid [8,17], and novel states with multiple vortices, or ''vortex clusters,'' will appear [9]. Quasiperiodic topological transformations within self-localized beams promise to bring many novel exciting phenomena.

Conclusions.—We have introduced novel classes of higher-order spatial optical solitons in the form of the soliton necklaces and soliton matrices stabilized by the nonlocal nonlinearity. These higher-order solitons represent generalization of the well-known Laguerre-Gaussian and Hermite-Gaussian linear modes in the case of nonlinear media. A rich variety of the stationary states found both analytically and numerically allows for nontrivial mutual transformations induced by modulational instability when the soliton powers become close or coincide. These soliton transformations are manifested as periodic robust oscillations between two or more spatially localized states with distinctly different symmetries.

This work has been supported by the Australian Research Council. The authors acknowledge useful discussions with Andrey Miroshnichenko.

[1] C. Conti, M. Peccianti, and G. Assanto, Phys. Rev. Lett. **92**, 113902 (2004); M. Peccianti, A. Dyadyusha, M. Kaczmarek, and G. Assanto, Nature Phys. **2**, 737 (2006).
[2] C. Rotschild, O. Cohen, O. Manela, M. Segev, and T. Carmon, Phys. Rev. Lett. **95**, 213904 (2005); C. Rotschild, B. Alfassi, O. Cohen, and M. Segev, Nature Phys. **2**, 769 (2006).
[3] W. Krolikowski and O. Bang, Phys. Rev. E **63**, 016610 (2000); W. Krolikowski, O. Bang, J. J. Rasmussen, and J. Wyller, *ibid.* **64**, 016612 (2001); J. Wyller, W. Krolikowski, O. Bang, and J. J. Rasmussen, *ibid.* **66**, 066615 (2002); O. Bang, W. Krolikowski, J. Wyller, and J. J. Rasmussen, *ibid.* **66**, 046619 (2002).
[4] D. Briedis, D. E. Petersen, D. Edmundson, W. Krolikowski, and O. Bang, Opt. Express **13**, 435 (2005); A. I. Yakimenko, Yu. A. Zaliznyak, and Yu. S. Kivshar, Phys. Rev. E **71**, 065603(R) (2005).
[5] S. Lopez-Aguayo, A. S. Desyatnikov, Yu. S. Kivshar, S. Skupin, W. Krolikowski, and O. Bang, Opt. Lett. **31**, 1100 (2006).
[6] S. Skupin, O. Bang, D. Edmundson, and W. Krolikowski, Phys. Rev. E **73**, 066603 (2006).
[7] A. I. Yakimenko, V. M. Lashkin, and O. O. Prikhodko, Phys. Rev. E **73**, 066605 (2006).
[8] A. S. Desyatnikov and Yu. S. Kivshar, Phys. Rev. Lett. **88**, 053901 (2002); A. S. Desyatnikov, A. A. Sukhorukov, and Yu. S. Kivshar, Phys. Rev. Lett. **95**, 203904 (2005).
[9] S. Lopez-Aguayo, A. S. Desyatnikov, and Yu. S. Kivshar, Opt. Express **14**, 7903 (2006).
[10] V. M. Lashkin, A. I. Yakimenko, and O. O. Prikhodko, nlin.PS/0607062.
[11] M. Soljacic and M. Segev, Phys. Rev. Lett. **86**, 420 (2001).
[12] C. Rotshild, M. Segev, Z. Xu, Y. V. Kartashov, L. Torner, and O. Cohen, Opt. Lett. **31**, 3312 (2006).
[13] Yu. S. Kivshar and G. P. Agrawal, *Optical Solitons* (Academic Press, San Diego, 2003), p. 540.
[14] A. S. Desyatnikov, Yu. S. Kivshar, and L. Torner, in *Progress in Optics*, edited by E. Wolf (North-Holland, Amsterdam, 2005), Vol. 47, p. 291, and references therein.
[15] V. A. Mironov, A. M. Sergeev, and E. M. Sher, Sov. Phys. Dokl. **26**, 861 (1981).
[16] E. G. Abramochkin and V. G. Volostnikov, J. Opt. A Pure Appl. Opt. **6**, S157 (2004).
[17] E. G. Abramochkin and V. G. Volostnikov, Phys. Usp. **47**, 1177 (2004).
[18] B. A. Malomed, in *Progress in Optics*, edited by E. Wolf (North-Holland, Amsterdam, 2002), Vol. 43, p. 71.
[19] J. J. García-Ripoll and V. Peŕez-García, SIAM J. Sci. Comput. **23**, 1316 (2001).
[20] Z. Xu, Y. V. Kartashov, and L. Torner, Opt. Lett. **30**, 3171 (2005).
[21] Yu. S. Kivshar, T. J. Alexander, and S. K. Turitsyn, Phys. Lett. A **278**, 225 (2001).